Available online at www.sciencedirect.com

SCIENCE DIRECT®

Earth and Planetary Science Letters 224 (2004) 157–174

EPSL

www.elsevier.com/locate/epsl

Precise Pt–Re–Os isotope systematics of the mantle from 2.7-Ga komatiites

Igor S. Puchtel[a,*], Alan D. Brandon[b], Munir Humayun[a]

[a] *Department of the Geophysical Sciences, The University of Chicago, 5734 S. Ellis Avenue, Chicago, IL 60637, USA*
[b] *NASA Johnson Space Center, Mail Code SR, Building 31, Houston, TX 77058, USA*

Received 8 January 2004; received in revised form 17 April 2004; accepted 30 April 2004
Available online 26 June 2004

Abstract

Precise Pt–Re–Os isotopic and highly siderophile element (HSE) data are reported for 10 drill core samples collected across a 2.7 m thick, differentiated komatiite lava flow at Pyke Hill in Ontario, Canada. The Pt–Re–Os isotopic data for five cumulate samples yield Re–Os and Pt–Os isochrons with ages of 2725 ± 33 and 2956 ± 760 Ma and initial $^{187}Os/^{188}Os = 0.10902 \pm 16$ and $^{186}Os/^{188}Os = 0.1198318 \pm 18$, respectively. These ages are consistent with the time of lava emplacement determined by other geochronometers. The initial $^{187}Os/^{188}Os$ isotopic composition of the Pyke Hill source is similar to the $^{187}Os/^{188}Os$ isotopic compositions of enstatite and ordinary chondrites and to that of PUM at 2725 Ma. Using the Pt–Os isotopic data for the Pyke Hill source, the present-day $^{186}Os/^{188}Os$ isotopic composition of PUM was calculated to be 0.1198387 ± 18. The regression of global $^{187}Os/^{188}Os$ isotopic data for terrestrial materials shown to represent Os isotopic composition of the contemporary mantle indicates that the LILE-depleted mantle evolved from the solar system starting composition and, over Earth's history, was on average ~ 8% depleted in Re vs. Os relative to PUM. From the HSE composition of the emplaced Pyke Hill komatiite lava, the mantle source was inferred to contain Re (0.30 ppb), Os (3.9 ppb), Ir (3.6 ppb), Ru (5.4 ppb), Pt (6.4 ppb), and Pd (6.3 ppb) in relative proportions similar to those in average enstatite chondrites, except for Pd, which was enriched over Pt by ~ 30% in the Pyke Hill source compared to enstatite chondrites. From these data, the $^{190}Pt/^{188}Os$ of PUM was calculated to be 0.00157. If the HSE abundances in the terrestrial mantle were inherited from chondritic material of a late veneer, the latter should have had the HSE composition of ordinary or enstatite chondrites. Alternatively, if the reenrichment of the mantle with HSE was the result of an open-system transport of material across the core–mantle boundary, it was likely a global event that should have occurred shortly after core formation.

Keywords: Pt–Re–Os; mantle isotope systematics; highly siderophile elements; Archean romatiites; Pyke Hill; late veneer

1. Introduction

The recent advances in N-TIMS and isotope dilution ICP-MS techniques have resulted in increasing use of the highly siderophile element (HSE) isotope geochronometers in mantle geochemistry. These provide a powerful analytical tool for studying

* Corresponding author. Present address: Department of Geology, University of Maryland, College Park, MD20742, USA.
E-mail address: ipuchtel@mail.umd.edu (I.S. Puchtel).

0012-821X/$ - see front matter © 2004 Elsevier B.V. All rights reserved.
doi:10.1016/j.epsl.2004.04.035

time-integrated variations in Re/Os and Pt/Os ratios within and between major terrestrial reservoirs (see reviews in [1,2]) by utilizing the $^{187}Re-^{187}Os$ and $^{190}Pt-^{186}Os$ decay schemes. The database on Re–Os isotope systematics of various types of modern upper mantle materials including mantle xenoliths [3], ophiolites [4], abyssal peridotites [5,6], MORBs [7,8], and orogenic massif lherzolites [9–11] has been rapidly expanding. Combined with the recently obtained Re–Os isotope data on several Archean to Paleozoic rock complexes shown to represent the composition of the contemporary upper to lower mantle [12–22], these results have demonstrated that the mantle on average has evolved with Re/Os ratios within 10% of those in chondrites. This has led many workers to put forward a hypothesis of a roughly chondritic evolution of both the convecting upper mantle (DMM: a hypothetical upper mantle reservoir that experienced a Re depletion as a result of previous episodes of melt extraction) and the primitive upper mantle (PUM: a hypothetical upper mantle reservoir that experienced no Re depletion) through time with DMM having some 1% to 2% less radiogenic $^{187}Os/^{188}Os$ isotopic composition than PUM [6]. The currently available $^{186}Os/^{188}Os$ isotope data on modern upper mantle materials are limited to those on abyssal peridotites, ophiolitic chromitites, and Os–Ir alloys [1,6,23]. When combined with the Pt–Os results for the carbonaceous chondrite Allende [1,24], these data indicated that the projected Pt/Os ratio of DMM has been on average within $\pm 30\%$ of a chondritic Pt/Os ratio over the Earth's history [6]. Estimates of the modern $^{186}Os/^{188}Os$ isotopic composition for PUM are not available, and there are currently no data with which to constrain the $^{186}Os/^{188}Os$ evolution of both DMM and PUM in the geological past. However, it is important to define the $^{186}Os/^{188}Os$ evolution curves of both DMM and PUM in the Precambrian in order to distinguish those from mantle reservoirs that have potentially derived their Os isotopic compositions from the outer core [1,25,26]. This information in turn can be used to constrain the timing of onset of crystallization and the growth rate of the inner core, a matter of considerable debate in global geophysics [27,28].

Recently, Puchtel et al. [29] described a precise technique for determining PGE abundances in Archean samples by the Carius tube digestion ID-ICP-MS technique and reported PGE abundances for three komatiite lava flows from the Alexo and Pyke Hill localities in Canada. In this study, precise Pt–Os and Re–Os isotopic data for one of the Pyke Hill komatiite flows are presented. Additional HSE abundance data for this flow have been obtained that complement those reported in [29]. The Pt–Os isotopic data for Pyke Hill komatiites are used to define the $^{186}Os/^{188}Os$ evolution curve for PUM and to discuss implications for models of Earth accretion, mantle differentiation, and core–mantle interaction. Lithophile data on the samples are presented to show that the Pyke Hill komatiite lavas have not been affected by crustal contamination, and to complement the HSE and Re–Pt–Os isotopic information.

2. Sampling

The Pyke Hill area is within the Abitibi greenstone belt (see Fig. 1 in [30]) in Munro Township, NE Ontario. Samples analyzed in this study came from a 2.7 m thick differentiated komatiite lava flow (PH-II; see Fig. 1 in [29]). This flow was chosen for this study because it had the highest Os abundances in its cumulate part and exhibited the lowest Pt/Os ratios, which are essential requirements for obtaining precise initial $^{186}Os/^{188}Os$ ratios in ancient rocks. The PH-II flow was sampled in the core S-97-07 drilled by Millstream Mines in 1997 and collared ~ 100 m west along strike from the outcrop described by Pyke et al. [31]. During the sampling, the entire core interval was taken and split into 10 samples. These included sample PH34 from the lower chilled margin, which was not analyzed by Puchtel et al. [29]. The flow is divided into an upper olivine spinifex (zone A) and a lower olivine cumulate (zone B) zone. Zone A is further divided into an upper chilled margin of aphanitic komatiite (subzone A_1) underlain by a random olivine spinifex-textured komatiite (subzone A_2). Zone B is divided into a thin B_1 subzone of elongated hopper olivine, and B_2 and B_4 subzones of olivine orthocumulate rock. Almost all olivine in the flow is altered to serpentine, chlorite, and magnetite, although clinopyroxene and chromite are well preserved.

3. Analytical techniques

During this study, the methodology repeatedly evolved as we defined the best means for combining high-precision $^{186}Os/^{188}Os$ isotopic compositions determined on unspiked digestions with elemental abundance ratios obtained on spiked aliquots from these digestions. The decision to carry out the Re–Os isotopic study was made after the Pt–Os data had been obtained and was performed on separate digestions of the same sample powder aliquots. For this study, three separate sets of digestions were performed for (1) HSE (PGEs and Re) abundance determinations, (2) $^{186}Os/^{188}Os$ isotope analyses on unspiked digestions and determination of Pt/Os ratios on spiked aliquots from the unspiked digestions, and (3) Re–Os isotope studies on spiked digestions. The sample preparation techniques and the analytical methods for PGE spike calibration, determination of major elements, minor elements, and PGE abundances are given in [29] and are only briefly described, where necessary, below.

3.1. HSE analysis

The procedure for analyzing Re by ID-ICP-MS was grafted on to the PGE procedure. The mixed PGE spike #000531 used in our komatiite studies (e.g., [29]) contains ^{185}Re, the concentration of which has been calibrated by both ICP-MS and N-TIMS against an in-house gravimetric standard produced by dissolving pure Re metal. The PGE analyses were carried out at The University of Chicago using the techniques of [29,32]. Samples were digested in 25-ml Pyrex™ borosilicate glass Carius tubes at 240 °C for 48–72 h. Several replicate digestions were performed at 270 °C for 48 h. After Os was extracted from the *aqua regia* sample solutions, these were dried, converted into the chloride form, taken up in 0.15*N* HCl, and Ir, Ru, Pt, Pd, and Re were separated from the matrix and further purified by cation exchange chromatography. The resulting eluate was used directly for ICP-MS analysis.

Measurements of Os, Ir, Ru, Pt, Pd, and Re isotopic compositions were performed on a Finnigan Element™ single-collector, magnetic sector, high-resolution ICP-MS at The University of Chicago. The sample solutions were introduced into the ICP-MS torch via a CETAC MCN6000 desolvating nebulizer for the PGE measurements. Experience with the MCN6000 showed that Re was volatilized by the desolvation process, producing erratic Re ion beams with significant memory effects. Consequently, an ESI™ low-flow nebulizer (100 μl/min) with ESI™ Teflon spray chamber was used for the Re measurements, which produced stable Re ion beams with a rapid (2 min) signal wash-out. Typical count rates were 10^5–10^6 cps for PGEs and 10^4–10^5 cps for Re, and the internal precisions of individual runs were better than 0.5% relative ($2\sigma_{aver}$). Long-term reproducibilities of 0.5 ppb in-house Ir–Ru–Pd–Pt and Re standard solutions and a 1 ppb Os standard solution, which characterize the external precision of the analysis, were 1–2% ($2\sigma_{stdev}$) on all isotope ratios. Mass fractionation for Ru, Pd, Ir, Pt, and Re was corrected using $^{99}Ru/^{102}Ru = 0.4044$, $^{110}Pd/^{106}Pd = 0.4288$, $^{191}Ir/^{193}Ir = 0.5942$, $^{198}Pt/^{195}Pt = 0.2130$, and $^{185}Re/^{187}Re = 0.5974$ relative to those measured in the standard solutions that were run alternately with samples. The measured $^{190}Os/^{192}Os$ ratios in the samples were corrected for fractionation using a linear law and $^{192}Os/^{188}Os = 3.083$. The total analytical blank was 5 pg Os, 0.5 pg Ir, 3 pg Ru, 31 pg Pt, 7 pg Pd, and 10 pg Re. Blank corrections applied were < 0.1% for Os, Ir, Ru, and Pd, ~ 0.3% for Pt, and < 1.5% for Re.

3.2. Pt–Os isotopic study

Chemical treatment of the samples for the Pt–Os isotopic study was carried out at The University of Chicago. To obtain the amount of osmium (~ 100 ng) required for the high-precision measurements of the $^{186}Os/^{188}Os$ isotopic composition, each of the five samples studied was processed in eight Carius tubes. No spike was added to the initial digestions, in which ~ 3 g of sample powder and ~ 13 ml of inverse *aqua regia* were placed into 25-ml Pyrex™ borosilicate glass Carius tubes, chilled to 0 °C, and sealed. The samples were digested at ~ 240 °C for 72–96 h. After the tubes were chilled and then opened, ~ 5% of the *aqua regia* sample solution from each of the eight Carius tubes was transferred into a new clean Carius tube for precise determination of the Pt/Os ratio. Before the transfer proce-

dure, the clean tube was chilled to 0 °C, and appropriate amount of the PGE spike #000531 was added to it, followed by ~5 ml of inverse *aqua regia* after the sample solution transfer was completed. This new tube was then sealed and kept in an oven at ~240 °C for 24 h to achieve sample–spike equilibration. After opening the tube, the spiked aliquot was processed using the same procedure utilized in the PGE analysis with one significant difference; without a knowledge of the precise weight of the sample represented by the amount of transferred solution, only the interelement ratios could be determined. However, only the Pt/Os ratio directly pertaining to the digested powder aliquot was of interest here and was obtained. From the remaining 95% of the unspiked *aqua regia* sample solution, Os was extracted and purified. The clean Os cuts from each of the eight CT unspiked digestions for the sample were combined into one cut and used for the precise measurements of the $^{186}Os/^{188}Os$ isotopic composition.

Measurements of Os and Pt isotopic compositions from the spiked aliquots, for the determination of precise Pt/Os ratios, were performed at The University of Chicago by ICP-MS. To achieve sufficient precision of the data, between 1200 and 2400 isotope ratios were collected for Os and Pt during each measurement. Otherwise, procedures of Puchtel et al. [29] were followed.

The high-precision measurements of the $^{186}Os/^{188}Os$ isotopic compositions were performed by N-TIMS in static mode on an eight-Faraday collector ThermoFinnigan Triton® mass spectrometer at the Johnson Space Center. Signals of 130–180 mV on mass 234 ($^{186}Os^{16}O_3^-$) and 235 ($^{187}Os^{16}O_3^-$) were generated for ≥180 ratios to reach the desired run precision of ±20 ppm or better ($2\sigma_{aver}$) for the $^{186}Os/^{188}Os$ ratio. The interference of $^{186}W^{16}O_3^-$ on $^{186}Os^{16}O_3^-$ was monitored by measuring $^{184}Os^{16}O_3^-$ ($^{184}W^{16}O_3^-$). The mean of 26 runs of the Johnson–Matthey Os standard during the analytical campaign was 0.0013092 ± 11 for $^{184}Os/^{188}Os$, 0.1198462 ± 21 for $^{186}Os/^{188}Os$, and 0.1137893 ± 45 for $^{187}Os/^{188}Os$ ($2\sigma_{stdev}$). Each sample load was run two to four times; the analytical uncertainties on Os isotope compositions are reported for each run, and the errors on averages are quoted at $2\sigma_{aver}$. To calculate the age, Pt–Os data were regressed using the ISOPLOT program [33] and the ^{190}Pt decay constant (λ) of 1.477×10^{-12} year^{-1} [34]. Error input was determined from the precision of the averages of the individual runs. All errors on age and initial isotopic ratios are quoted at $2\sigma_{aver}$. The initial $^{186}Os/^{188}Os$ of a particular sample was calculated from its measured Os isotopic composition and the Pt/Os ratio:

$$\left(\frac{^{186}Os}{^{188}Os}\right)_i^{sample} = \left(\frac{^{186}Os}{^{188}Os}\right)_{measur}^{sample} - \left(\frac{^{190}Pt}{^{188}Os}\right)_{measur}^{sample} \times \left(e^{\lambda T} - 1\right)$$

3.3. Re–Os isotope study

For a more direct comparison between Pt–Os and Re–Os systematics, it was decided to also study the Re–Os isotopic compositions of each sample used in the Pt–Os study. Chemical treatment of the samples for the Re–Os study was performed at The University of Chicago. Digestion procedures of the samples, as well as Os extraction and purification procedures, were identical to those used in the PGE analysis. Rhenium was recovered from the residual *aqua regia* solution and purified by anion exchange chromatography. A 2-ml glass column filled with Bio-Rad® AG 1-X8 resin was used to separate Re from the bulk of the rock matrix. A second 200-μl Teflon column was used for purification of the Re fraction.

Precise isotopic compositions of Os and Re were measured in static mode via N-TIMS on the ThermoFinnigan Triton® mass spectrometer at the Johnson Space Center. Both Os and Re isotopic data were collected using Faraday cups. The effects of fractionation during Os runs were eliminated by normalizing the Os isotope ratios to $^{192}Os/^{188}Os = 3.083$. Measured Re isotopic ratios were not corrected for fractionation, which was estimated to be negligible based on the data for the in-house Re standard ($^{187}Re/^{185}Re = 1.6733 \pm 19$). The total analytical blank was ~10 pg Re and ~5 pg Os. Blank corrections applied were ~0.1% for Os and <1.8% for Re. Analytical uncertainties on Re and Os isotope compositions are reported for each sample. To calculate the age, Re–Os data were regressed using the ISOPLOT program [33]. Error input was determined from the in-run precision of

Table 1
Re–Os isotopic data

Sample	Re (ppb)	Os (ppb)	Re/Os	$^{187}Re/^{188}Os$	$^{187}Os/^{188}Os$	$\gamma^{187}Os$ (T)
PH29	0.4813	4.034	0.119	0.5754 ± 58	0.135620 ± 21	0.50
PH30	0.3011	7.238	0.042	0.2002 ± 30	0.118275 ± 20	0.58
PH31	0.2253	7.480	0.030	0.1449 ± 27	0.115730 ± 21	0.60
PH32	0.3786	5.902	0.064	0.3089 ± 40	0.123550 ± 16	0.79
PH33	0.3926	4.701	0.084	0.4024 ± 44	0.127700 ± 26	0.61

The data obtained by N-TIMS on separate 2-g digestions. The $\gamma^{187}Os$ values for individual samples calculated at $T=2725$ Ma. The Re and Os abundances are recalculated on an anhydrous basis.

the individual Os isotopic analyses. All errors on age and initial isotopic ratios are quoted at $2\sigma_{aver}$. The initial $\gamma^{187}Os$ value was calculated as the percent deviation of the isotopic composition at the time defined by the isochron relative to the chondritic reference at that time [2]. The initial $^{187}Os/^{188}Os$ of a particular sample was calculated from its measured Os isotopic composition and Re/Os ratio:

$$\left(\frac{^{187}Os}{^{188}Os}\right)_i^{sample} = \left(\frac{^{187}Os}{^{188}Os}\right)_{measur}^{sample} - \left(\frac{^{187}Re}{^{188}Os}\right)_{measur}^{sample} \times \left(e^{\lambda T} - 1\right)$$

The average chondritic Os isotopic composition at the time T defined by the isochron was calculated using the ^{187}Re decay constant (λ) of 1.666×10^{-11} year^{-1}, the starting solar system $^{187}Os/^{188}Os = 0.09531$, and the present-day average chondritic composition ($^{187}Re/^{188}Os = 0.40186$, $^{187}Os/^{188}Os = 0.1270$; [2,35]):

$$\left(\frac{^{187}Os}{^{188}Os}\right)_i^{CHON} = 0.09531 + 0.40186\left(e^{\lambda 4.558} - e^{\lambda T}\right)$$

3.4. Lithophile trace element analysis

The abundances of lithophile trace elements were determined on an ELAN 6100 DRC ICP-MS at the Institute of Geochemistry of Trace Elements in Moscow. Mixed REE spike was added to the samples before digestion. Samples were digested in closed Teflon® vials in a Multiwave® microwave oven at 260 °C in a mixture of double-distilled concentrated HF, HNO_3, and $HClO_4$ acids. After digestion, the sample solutions were split into two parts. One part after dilution was directly used for

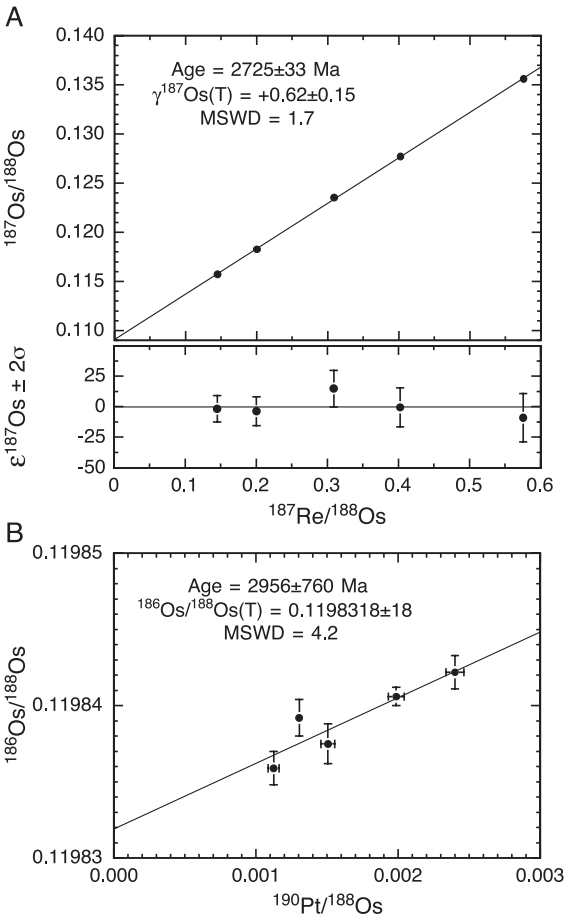

Fig. 1. Re–Os (A) and Pt–Os (B) isochron diagrams for the PH-II lava flow. The Pt–Os age was calculated using the ^{190}Pt decay constant (λ) of 1.477×10^{-12} year^{-1} [34].

the analysis of all trace elements, except REE. From the second part, REE were separated and further purified using cation exchange chromatography. The accuracy of the analyses was estimated to be ~1% (relative) for REE and ~3–5% for the rest of trace elements and was determined by multiple analyses of USGS standards BCR, BHVO, and BIR.

4. Results

4.1. Pt–Os and Re–Os isotope data

The Re–Os isotopic data for the five cumulate samples analyzed are presented in Table 1 and plotted on the $^{187}Re/^{188}Os$ vs. $^{187}Os/^{188}Os$ isochron diagram in Fig. 1A. Regression of the data yields an isochron with an age of 2725 ± 33 Ma and an initial $^{187}Os/^{188}Os$ of 0.10902 ± 0.00016, corresponding to $\gamma^{187}Os(T) = +0.62 \pm 0.15$.

The precise Os isotopic compositions and the corresponding Pt/Os ratios for the five cumulate samples analyzed are listed in Table 2 and plotted on the $^{190}Pt/^{188}Os$ vs. $^{186}Os/^{188}Os$ isochron diagram in Fig. 1B. The data define a regression line with a slope corresponding to an age of 2956 ± 760 Ma and an initial $^{186}Os/^{188}Os$ of 0.1198318 ± 18 using the ^{190}Pt decay constant of 1.477×10^{-12} year^{-1} [34]. High precision $^{187}Os/^{188}Os$ ratios determined in the Pt–Os study differ by 0.2–8.6% from those determined in the Re–Os study. This difference is likely a measure of sample powder homogeneity and is similar to the difference in the Re/Os ratios determined in the Re–Os isotope study and in the HSE abundance study.

4.2. Highly siderophile element abundances

The PGE and Re abundances for all 10 samples from the PH-II flow determined by IDθICP-θMS are listed in Table 3 and plotted in the MgO variation diagrams in Fig. 2. Also plotted are data for an olivine separate from sample PH30. The Re and Os abundances determined separately by N-TIMS (Table 1) and by ID-ICP-MS (Table 3) in the same samples agree to within 1–7%, whereas the Re/Os ratios agree to within 4% excluding PH31 (10%). The Pt/Os ratios determined by ID-ICP-MS in the same samples for both the HSE abundance study and the Pt–Os isotope study agree to within 2–14%. This large range of variation of Pt/Os ratios observed between replicate

Table 2
Precise Os isotopic data and Pt–Os abundance ratios

Sample	Pt/Os	$^{190}Pt/^{188}Os$	$^{184}Os/^{188}Os$	$^{186}Os/^{188}Os$	$^{187}Os/^{188}Os$
PH29			0.0013074 ± 09	0.1198409 ± 14	0.1347940 ± 17
			0.0013118 ± 11	0.1198420 ± 17	0.1347956 ± 17
			0.0013096 ± 08	0.1198435 ± 12	0.1347906 ± 13
			0.0013099 ± 16	0.1198425 ± 19	0.1347933 ± 22
Average	2.520 ± 54	0.002407 ± 52	0.0013097 ± 18	0.1198422 ± 11	0.1347934 ± 21
PH30			0.0013120 ± 11	0.1198410 ± 17	0.1192962 ± 17
			0.0013074 ± 12	0.1198386 ± 18	0.1192957 ± 20
			0.0013099 ± 12	0.1198387 ± 16	0.1192979 ± 18
			0.0013116 ± 11	0.1198386 ± 20	0.1192973 ± 17
Average	1.371 ± 23	0.001310 ± 22	0.0013102 ± 21	0.1198392 ± 12	0.1192968 ± 10
PH31			0.0013099 ± 07	0.1198348 ± 15	0.1152769 ± 13
			0.0013076 ± 07	0.1198366 ± 12	0.1152762 ± 12
			0.0013083 ± 08	0.1198363 ± 13	0.1152755 ± 12
Average	1.181 ± 29	0.001128 ± 28	0.0013086 ± 13	0.1198359 ± 11	0.1152762 ± 08
PH32			0.0013075 ± 11	0.1198368 ± 17	0.1225529 ± 17
			0.0013099 ± 12	0.1198381 ± 19	0.1225256 ± 17
Average	1.582 ± 30	0.001511 ± 29	0.0013087 ± 24	0.1198375 ± 13	0.122539 ± 27
PH33			0.0013104 ± 12	0.1198409 ± 17	0.1277365 ± 34
			0.0013078 ± 11	0.1198403 ± 17	0.1277231 ± 25
Average	2.086 ± 21	0.001993 ± 20	0.0013091 ± 26	0.1198406 ± 06	0.127730 ± 13

The Os isotopic compositions were determined by N-TIMS on 24-g unspiked digestions. The Pt–Os ratios were determined by ID-ICP-MS on spiked aliquots obtained by postdissolution subsampling of the 24-g unspiked digestions.

Table 3
PGE and Re concentrations (ppb)

Sample	Re	Os	Ir	Ru	Pt	Pd	$(Os/Ir)_N$	Re/Os	Pt/Os	Pd/Pt	Pt/Re
PH25		2.54	2.26	5.06	10.6	10.2	1.06		4.16	0.96	
PH25[a]		2.58	2.33	5.45	10.8	10.6	1.05		4.19	0.98	
PH25[a]	**0.450**	**2.73**	**2.36**	**5.39**	**11.4**	**10.6**	**1.09**	**0.165**	**4.18**	**0.93**	**25.3**
PH26		1.98	1.76	4.73	10.8	10.4	1.06		5.45	0.96	
PH26[a]	**0.457**	**1.88**	**1.69**	**5.16**	**10.9**	**10.9**	**1.05**	**0.244**	**5.79**	**1.00**	**23.8**
PH27		1.72	1.59	4.99	10.9	10.8	1.02		6.34	0.99	
PH27[a]	**0.464**	**1.71**	**1.56**	**5.32**	**11.3**	**10.8**	**1.04**	**0.272**	**6.61**	**0.96**	**24.3**
PH28		1.73	1.64	4.90	11.1	10.9	1.00		6.42	0.98	
PH28[a]	**0.524**	**1.90**	**1.69**	**5.23**	**11.9**	**11.2**	**1.06**	**0.276**	**6.30**	**0.94**	**22.8**
PH29		4.29	3.61	5.64	9.67	9.67	1.12		2.26	1.00	
PH29[a]	**0.471**	3.92	3.20	5.26	9.41	9.37	1.16	**0.120**	2.40	1.00	**20.0**
PH30		5.89	4.61	5.64	7.98	7.93	1.21		1.35	0.99	
PH30[a]	**0.291**	6.97	5.45	5.48	8.26	7.75	**1.21**	**0.042**	1.18	0.94	**28.4**
PH31		7.61	6.00	5.69	8.11	7.93	1.20		1.07	0.98	
PH31[a]	**0.243**	7.23	5.42	5.59	8.22	7.59	1.26	**0.034**	1.14	0.92	**33.8**
PH32		5.15	4.23	5.37	8.51	8.36	1.15		1.65	0.98	
PH32[a]	**0.370**	5.54	4.31	5.31	8.59	8.06	1.21	**0.067**	1.55	0.94	**23.2**
PH33		4.78	3.78	5.53	8.78	9.10	1.19		1.84	1.04	
PH33[a]	**0.381**	4.74	3.42	5.17	8.92	8.88	1.31	**0.080**	1.88	0.99	**23.4**
PH34	**0.490**	**2.15**	**1.95**	**5.33**	**11.4**	**10.8**	1.04	**0.228**	**5.29**	**0.95**	**23.2**
PH30 Ol	**0.050**	**1.35**	**0.956**	**3.16**	**0.256**	**0.413**	**1.33**	**0.037**	**0.190**	**0.62**	**5.07**

Boldfaced values—data from this study, obtained by the CT-digestion ID-ICP-MS technique. Digestions performed at 270 °C for 48 h after preheating at 240 °C for 24 h. Data on the same samples from [29] are shown for comparison. All analyses recalculated on an anhydrous basis.
[a] Replicate digestions of same sample powder aliquots.

analyses of the same samples necessitated the determination of precise Pt/Os ratios on the same 24-g digestions that were performed for the Pt–Os isotopic study.

The two chilled margin samples that represent composition of the emplaced komatiite lava contain on average 2.4 ppb Os, have suprachondritic (Os/Ir) $N = 1.1$ and are enriched in IPGEs over PPGEs [(Pd/Ir) $N = 4.3$]. The Pt and Pd abundances in the lava plot on tight trends that pass through the measured olivine compositions and thus represent olivine fractionation/accumulation lines. This type of correlation indicates a strongly incompatible behavior during lava differentiation that was solely controlled by olivine [29]. The Re abundances for all, but two most magnesian cumulate samples, also plot on an olivine control line indicating a similarly incompatible behavior during lava differentiation. In contrast to Re, Pt, and Pd, the abundances of Os, Ir, and Ru plot on trends with positive slopes and well above the olivine compositions. This indicates that fractionation of Os, Ir, and Ru in the lavas was controlled by an IPGE-rich phase and the olivine [29]. The trend for Ru has only a slight slope, indicating that this element was little affected during lava differentiation. The inverse behavior of Os and Re–Pt during magmatic lava differentiation resulted in up to 10× variations in the Re/Os and Pt/Os ratios (0.030–0.28 and 1.1–6.6, respectively) over the range of MgO abundances in the samples (Fig. 3).

5. Discussion

5.1. Pt–Os and Re–Os systematics and the initial Os isotopic composition of the mantle source

In order to determine whether the initial Os isotopic compositions of the Pyke lavas are representative of those in their mantle source, it is necessary to compare the ages defined by the two HSE geochronometers with the existing geochronological information on the Pyke Hill lavas. The U–Pb zircon ages of the felsic lavas underlying and overlying the komatiites at Pyke Hill range between 2715 ± 2 and 2703 ± 2 Ma [36]. The Sm–Nd age of komatiites

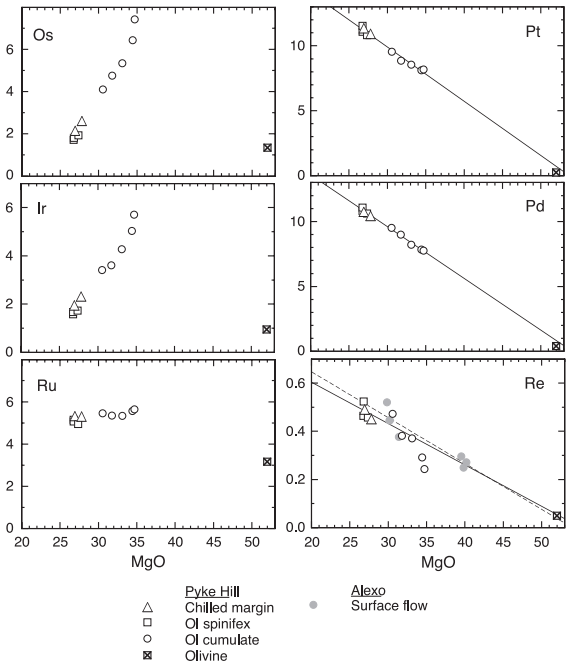

Fig. 2. Variation diagrams of MgO (wt%) vs. PGEs and Re (ppb) for the PH-II lava flow. The Re data for the Alexo surface flow from [19] are shown for comparison. The trends are best fit lines drawn linear law (Pt, Pd, Re) through the data points.

calculated from the published data [37–39] is 2713 ± 29 Ma with $\varepsilon Nd(T) = +2.9 \pm 0.2$. Finally, Pb–Pb isotope studies of Pyke Hill komatiites produced an isochron with an age of 2746 ± 56 Ma and $\mu_1 = 8.6 \pm 0.1$ [40]. Thus, the Re–Os isochron age of the PH-II flow is consistent with the emplacement age of komatiite lavas at Pyke Hill derived from the lithophile element isotope systems. This implies that either the Re–Os system has remained closed after the lava emplacement or it was disturbed during or shortly after emplacement and remained intact ever since. These two scenarios can be constrained using the Re and Os variations in the lavas. During komatiite lava differentiation, Re, similarly to Pt and Pd, behaves as an incompatible element. This is due to its incompatibility in olivine, as evidenced by the very low Re content in the olivine separate ($D^{Ol\text{-}Liq}_{Re} = 0.1$; Table 3) and by the experimental data [41,42]. As such, a magmatic behavior of Re in a given komatiite lava flow would require that Re abundances plot on an olivine control line, and any deviation from this line should be treated as evidence for Re mobility. The fact that the Re data for PH-II generally follow the olivine control line (Fig. 2) favors the former interpretation. Interestingly, the trend for the Pyke Hill samples overlaps with the trend for Alexo komatiites that we generated using the Re data of Gangopadhyay and Walker [19]. Furthermore, Os, as well as other PGE abundances, varies in a regular fashion in the lava flow (Fig. 2), consistent with these variations being controlled by magmatic differentiation. This indicates that Re and Os in the flow were immobile during secondary alteration, as was also concluded by Puchtel et al. [29] on the basis of their study of a larger set of samples from Pyke Hill and Alexo. Thus, the combination of immobile behavior of Re and Os, and the fact that the Re–Os isotopic data yield an isochron, indicates that the initial $\gamma^{187}Os(T)$ of $+0.62 \pm 0.15$ defined by the isochron corresponds to that in the original Pyke Hill komatiite lavas. It should be noted that two most MgO–rich cumulates (PH30 and PH31) plot below the olivine control line in Fig. 2. Although Re in these samples may have been disturbed, the fact that these samples plot on the same isochron indicates that such disturbance should have occurred during or shortly after lava emplacement.

Some komatiites are known to have assimilated large quantities of continental crustal material (e.g., [43]), and this may result in a more radiogenic Os isotopic composition of the lavas compared to that in their source (see discussion in [17]). However, the effects of crustal contamination can be easily detected using lithophile element systematics (e.g., [44]). The lithophile element geochemical characteristics of the

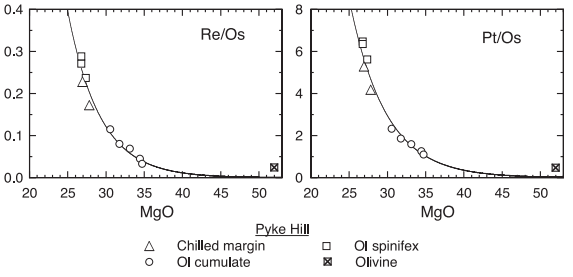

Fig. 3. Variation diagrams of MgO (wt.%) vs. Re/Os and Pt/Os ratios for the PH-II lava flow. The trends are best fit lines drawn exponential law through the data points.

PH-II flow, including high-MgO abundances (27.4%), which are at the high-end of the range of MgO contents observed in the emplaced Archean komatiite lavas worldwide (26–29%; [45]), the strong depletion in LILE, the positive Nb anomalies (Fig. A2; Table A1), radiogenic Nd – [εNd(T)= + 2.9] and unradiogenic Pb isotopic compositions ($\mu_1 = 8.6$) are strong evidence that these lavas are primary mantle melts that have not experienced any contamination by material of either continental crust or subcontinental lithospheric mantle. Consequently, the PH-II flow initial γ^{187}Os is considered to reflect that in its mantle source.

The Pt–Os age obtained in this study is identical, within the analytical uncertainty, to the emplacement age of the Pyke Hill lavas, but is significantly less precise. The large error on the age is due to the very narrow range in the ^{190}Pt/^{188}Os ratios (0.0011–0.0024) in the samples studied (Table 2), the low atomic abundance of ^{190}Pt, and its extremely small decay constant. To put this in perspective, the ^{190}Pt/^{188}Os ratios in the 250 Ma Noril'sk ores, which define an isochron precise enough to calculate the decay constant of ^{190}Pt [1], vary between 0.0013 and 172, i.e., by more than five orders of magnitude. However, the error on the calculated initial ^{186}Os/^{188}Os in the PH-II flow is small due to the low ^{190}Pt/^{188}Os ratios in the samples and high precision of the measurements, which resulted in a minimal error propagation from the extrapolation towards Pt/Os = 0 in the isochron diagram (Fig. 1). Similarly to the Re–Os systematics, the fact that the Pt–Os data define an isochron, coupled with the evidence for immobile behavior of Pt and Os during alteration, indicates that the initial ^{186}Os/^{188}Os of the lava corresponds to that in its mantle source.

As the regression line obtained is effectively the first Archean Pt/Os isochron and has an important bearing on the evolution of the ^{186}Os/^{188}Os isotopic composition of the contemporary mantle, it is important to consider various factors that could have led to obtaining a biased result. Because secondary alteration and contamination of the lavas have been ruled out, other possibilities need to be addressed. One potential concern might be that the samples were not completely digested, and therefore not all Os and Pt carriers were accessed. As perhaps the most resistant phases to digest in Carius tubes include chromite and Os–Ir alloys, which have Pt/Os ratios lower than those in the bulk rocks and thus contain less radiogenic Os; incomplete digestion of these phases would result in more radiogenic measured Os isotopic compositions. However, as long as individual phases in the sample are in isotopic equilibrium with the bulk rock (for example, the isotopic system has not been disturbed since the time of lava emplacement on the scale of the samples), and as far as determinations of Pt/Os ratios have been performed on the same digestions, incomplete dissolution of resistant phases only moves the whole rock analyses along the isochron, having no effect on the slope of the regression line and thus on the calculated initial isotopic composition. Furthermore, the study by Puchtel et al. [29] and also this work provide evidence for quantitative extraction of Os, Pt, and other PGEs during Carius tube sample digestions. First, replicate digestions performed at different temperatures (240 and 270 °C) gave consistent results for all PGEs (Table 3). Second, Puchtel et al. [29] demonstrated by time/temperature-series experiments for KAL-1 komatiite and GP-13 peridotite standards that the Os, Ir, Ru, Pt, and Pd abundances, obtained by methods used herein, do not reflect incomplete digestion, and that their data are consistent with those obtained in other laboratories using both CT and HPA digestions. We conclude therefore that the initial ^{186}Os/^{188}Os derived from the Pt–Os isochron reflects that in the source of the Pyke Hill komatiite lavas.

In Fig. 4, the ^{187}Os/^{188}Os isotopic compositions of Pyke Hill komatiites from this study together with the averages for ophiolitic chromitites [4], abyssal peridotites [6], carbonaceous, enstatite, and ordinary chondrites [24,46], estimates for PUM from the global study on mantle xenoliths [47], and the solar system initial [2] are plotted against time. A regression line through SSI and the Pyke Hill source intersects the zero time barrier at ^{187}Os/^{188}Os = 0.1293. This composition is identical to that of PUM (0.1296 ± 0.0008) and requires that the Pyke Hill source evolved with a ^{187}Re/^{188}Os = 0.4308. This ratio is ~ 7% higher than that in the chondritic reference (0.4019; [2]) and ~ 9% higher than that in an average carbonaceous chondrite (0.3932) calculated from the data of Walker et al. [46] and Brandon [24]. However, this ratio is within 2–4% of that in average enstatite (0.4226) and ordinary (0.4148) chondrites. As can be also seen from Fig. 4, abyssal peridotites, which represent the

composition of depleted upper mantle (DMM), have less radiogenic $^{187}Os/^{188}Os$ isotopic compositions than the source of the Pyke Hill lavas.

One of the uncertainties in calculating the precise initial $^{186}Os/^{188}Os$ of the source of the Pyke Hill komatiites is the value of the ^{190}Pt decay constant. Three different values of this constant are currently available. Walker et al. [1] obtained a value of the decay constant of 1.542×10^{-12} year^{-1} from a precise isochron on Noril'sk ores. This value was revised to 1.477×10^{-12} year^{-1} by Begemann et al. [34] using a more accurate ^{190}Pt atomic abundance of 0.01292% from Morgan et al. [48]. Subsequently, Cook et al. [49] obtained a value of 1.415×10^{-12} year^{-1} from a Pt–Os isochron on IIIAB iron meteorites. Either of the last two numbers is a reasonable representation of the value obtained by intercalibrating the U–Pb decay system with the ^{190}Pt–^{186}Os decay system. In this study, we use the decay constant of Begemann et al. [34].

The present-day $^{186}Os/^{188}Os$ and $^{190}Pt/^{188}Os$ ratios for DMM were established by Walker et al. [1] and Brandon et al. [6,25] to be 0.1198350 ± 10 and 0.00174, respectively, on the basis of their measurements of abyssal peridotites and ophiolitic Os–Ir alloys and chromitites. These results are very similar to those for the Allende carbonaceous chondrite [1,24]. This composition of modern DMM projects to the solar system initial $^{186}Os/^{188}Os$ ratio of 0.1198232 ± 10. Using the value of $^{186}Os/^{188}Os = 0.1198350 \pm 10$ as a proxy for the present-day $^{186}Os/^{188}Os$ isotopic composition of DMM, and calculating the mantle evolution curve, it can be shown that an average Pyke Hill initial $^{186}Os/^{188}Os$ ratio at 2725 Ma of 0.1198323 ± 9 ($2\sigma_{aver}$) plots 42 ± 20 ppm above the DMM evolution curve (Fig. 5). At this point, it is not quite clear if the Pyke Hill source had a more radiogenic $^{186}Os/^{188}Os$ isotopic composition relative to chondrites, as the $^{186}Os/^{188}Os$ isotopic data for chondrites are limited to those for Allende (carbonaceous), Chainpur (ordinary), and Indarch (enstatite) [1,24]. However, the elevated $^{186}Os/^{188}Os$ ratio of the Pyke Hill source, relative to DMM, is consistent with its $^{187}Os/^{188}Os$ isotopic composition, which is about 1.5 gamma units more radiogenic than DMM. To put this in perspective, the sources of the Siberian [1] and Hawaiian and Gorgona plumes [25,26] have $^{186}Os/^{188}Os$ isotopic ratios

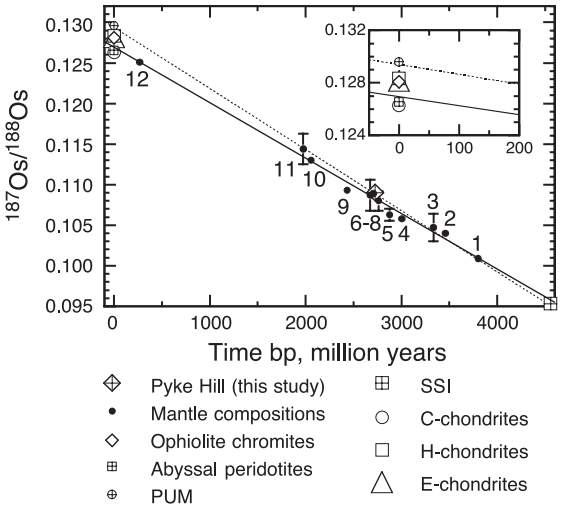

Fig. 4. Evolution diagram of $^{187}Os/^{188}Os$ vs. time for selected mantle-derived materials and chondrites. The dotted line represents the regression line through the SSI composition [2] and that of the Pyke Hill source. The solid line represents the best fit line through the compositions of mantle-derived materials: 1—Greenland peridotites, 2—Pilbara komatiites, 3—Commondale boninites, 4—Olondo peridotites, 5—Ruth Well komatiites, 6—Alexo komatiites, 7—Kambalda komatiites and sulfides, 8—Pyke Hill komatiites, 9—Vetreny Belt komatiites, 10—Finnish Lapland komatiites, 11—Onega plateau peridotites, 12—Vietnam komatiites. See text for references.

that are up to 150 ppm higher than modern DMM (Fig. 5), and their $^{187}Os/^{188}Os$ isotope compositions are up to eight gamma units higher than in modern DMM.

Whereas the $^{187}Os/^{188}Os$ isotopic composition of the primitive upper mantle (PUM) has been recently established [47], a complementary study on the $^{186}Os/^{188}Os$ isotopic composition of mantle xenoliths has yet to be performed to characterize the Pt–Os isotopic systematics of PUM. As the mantle source of the Pyke Hill komatiites had $^{187}Os/^{188}Os$ isotopic composition identical to that in PUM, the Pt–Os isotopic data for the Pyke Hill source might be used to infer the $^{186}Os/^{188}Os$ composition of PUM, pending $^{186}Os/^{188}Os$ measurements on mantle xenoliths. The $^{190}Pt/^{188}Os$ ratio of the source for the Pyke Hill komatiites calculated from the HSE data is 0.000157 (Table 5). Taking the initial from the isochron of 0.1198318 ± 18 and allowing the source to evolve to the present, gives a present-day $^{186}Os/^{188}Os$ ratio of

the source of 0.1198387 ± 18. Alternatively, taking the average initial at 2725 Ma of 0.1198323 ± 9 (Table 4), it can be shown that the source at present would have a nearly identical $^{186}Os/^{188}Os$ ratio of 0.1198386 ± 9. Hence, the present-day $^{186}Os/^{188}Os$ isotopic composition of PUM derived from the Pt–Os isotope systematics of the Pyke Hill komatiites is 0.1198387.

5.2. Implications for the $^{187}Os/^{188}Os$ isotopic evolution of the terrestrial mantle

Recent advances in the negative thermal ionization mass spectrometry technique have resulted in a rapid expansion of high-quality $^{187}Os/^{188}Os$ isotopic database for various types of mantle-derived materials including mantle nodules [47], abyssal peridotites [5,6], ophiolites [4], and mafic–ultramafic lavas (e.g., [17,18,26,50]). Among these materials, ophiolites and komatiites range in age between 3.8 and 0.08 Ga and thus cover more than two-thirds of the Earth's history. A quick examination of the available database reveals a bimodal distribution of $^{187}Os/^{188}Os$ isotopic compositions. The majority of rocks scatter along the chondritic reference line of Shirey and Walker [2] indicating their derivation from sources that evolved with time-integrated near-chondritic Re/Os ratios. There are however some notable excursions from this trend. Some plume-derived mafic–ultramafic lavas have radiogenic $^{187}Os/^{188}Os$ isotopic compositions that indicate that their respective sources evolved with time-integrated suprachondritic Re/Os ratios (e.g., [25,50–55]). These radiogenic Os isotopic compositions plot on or near the model outer core evolution curve and are largely interpreted to have been derived from the outer core [56], although some enrichments are attributed to the contribution of radiogenic Os from recycled oceanic crust (e.g., [57]). On the other hand, some materials reveal unradiogenic Os isotopic compositions [16,58] that were inferred to have been derived from sources that evolved with time-integrated subchondritic Re/Os ratios, e.g., from subcontinental lithospheric mantle.

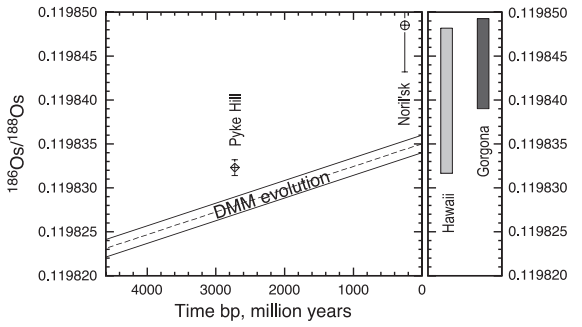

Fig. 5. Average $^{186}Os/^{188}Os$ isotopic composition of Pyke Hill komatiites recalculated at the time of the lava emplacement (2725 Ma) using a ^{190}Pt decay constant of Begemann et al. [34]. The evolution trend for the $^{186}Os/^{188}Os$ isotopic composition of DMM was calculated using the present-day $^{186}Os/^{188}Os = 0.1198350 \pm 10$ and $^{190}Pt/^{188}Os = 0.00174$ [1,6,25], and a ^{190}Pt decay constant of Begemann et al. [34]. The data for the Siberian [1], Hawaiian [25], and Gorgona plumes [26] are shown for comparison.

In order to trace the $^{187}Os/^{188}Os$ isotopic evolution of the mantle over geological time, the available database for mafic–ultramafic lavas and related rocks was filtered to select the well-studied localities, for which accurate Os isotopic compositions unambiguously shown to reflect those of contemporary mantle have been determined. These include (in the order of decreasing age) 3.8-Ga spinel peridotites of SW Greenland and 3.46-Ga komatiites of Pilbara region in W. Australia [18], 3.33-Ga boninites from the Commondale greenstone belt in S. Africa [21], 3.0-Ga peridotites from the Olondo ophiolite in the Aldan Shield [59], 2.88-Ga komatiites from the Ruth Well area in Australia [3], 2.72-Ga komatiites from the Alexo and Pyke Hill areas in Canada ([14,19]; this study), 2.70-Ga komatiites from Kambalda in Australia [13], komatiites from the 2.43-Ga Vetreny belt in the Baltic Shield [17], 2.0-Ga komatiites from Finnish Lapland [22], peridotites from the 2.0-Ga Onega plateau in the Baltic Shield [15], and 0.27-Ga komatiites from Vietnam [20]. On the $^{187}Os/^{188}Os$ vs. time diagram in Fig. 4, these data plot along a well-defined trend ($r = 0.995$), which gives intercepts at $^{187}Os/^{188}Os = 0.09565 \pm 0.00038$ ($T = 4558$ Ma) and 0.1271 ± 0.0005 ($T = 0$ Ma). The lower intercept is identical within uncertainty to the SSI of 0.09531 ±0.00011 [2]. The present-day intercept of 0.1271 ±0.0005 is identical to the chondritic reference of 0.1270 [2]. These data indicate that the upper mantle over the Earth's history evolved from the SSI $^{187}Os/^{188}Os$ composition with $^{187}Re/^{188}Os =$ 0.4020. It was therefore ~ 8% depleted in Re vs. Os relative to PUM.

Table 4
Pt–Os isotopic compositions of Pyke Hill komatiites and the mantle

Sample	$^{190}Pt/^{188}Os$	$^{186}Os/^{188}Os$	Initial [1]
PH29	0.00241	0.1198422	0.1198325
PH30	0.00131	0.1198392	0.1198339
PH31	0.00113	0.1198359	0.1198313
PH32	0.00151	0.1198375	0.1198314
PH33	0.00199	0.1198406	0.1198326
Average			0.1198323 ± 9
DMM	0.00174	0.1198350 ± 10	0.1198280 ± 10

The initial $^{186}Os/^{188}Os$ isotopic compositions were calculated at $T = 2725$ Ma using a ^{190}Pt decay constant of 1.477×10^{-12} year^{-1} [34]. The parameters for DMM from [1,6,25].

5.3. HSE composition of the Pyke Hill source and LILE and Re depletions in the mantle

The $^{187}Re–^{188}Os$ and $^{190}Pt–^{188}Os$ isotope systematics of the Pyke Hill komatiites indicate that the mantle source of the lavas evolved with time-integrated near-chondritic Re/Os and Pt/Os ratios. However, the instantaneous values of these ratios cannot be constrained in this manner, as any changes in the Re/Os and Pt/Os ratios of the source shortly before the komatiite lava formation will not be detectable due to the very slow radiogenic ingrowth of the daughter isotopes. Therefore, we calculated the HSE abundances in the Pyke Hill source using those in the emplaced Pyke Hill komatiite lava. The techniques and assumptions applied in this modeling were outlined by Puchtel et al. [29]. In short, the abundances of Pt and Pd were constrained from the regressions with MgO (Fig. 2) and assuming that the MgO in the source (38.3%) was similar to that in an average depleted spinel lherzolite (ADSL; [29]). This was possible due to incompatible behavior of Pt and Pd during high degrees of partial melting and magma differentiation. The Ru abundance and the Os/Ir ratio in the source were inferred from the partitioning behavior to be identical to those in the emplaced komatiite lava, and the Ru/Ir ratio was taken to be chondritic, so that the absolute IPGE abundances in the source were determined by Ru. Here, similarly to the Pt and Pd abundances in the source, the concentration of incompatible Re in the source was calculated from the Re vs. MgO regression (Fig. 2). The results of the calculations are summarized in Table 5 and plotted in Fig. 6. The calculated Pyke Hill source has near-CI-chondritic relative abundances of Re, Os, Ir, Ru, and Pt and is ~50% enriched in Pd. As expected, the calculated mantle residue left after ~50% melting and extraction of the Pyke Hill komatiite (Fig. 6A) was depleted in Re, Pt, and Pd and was slightly enriched in Os and Ir. From the inferred Pt and Os abundances in the Pyke Hill source, the $^{190}Pt/^{188}Os$ ratio of PUM was calculated to be 0.00157.

The Pyke Hill komatiites and hence their mantle source are characterized by strong LILE depletions (Table A1). These depletions and the radiogenic Nd isotopic composition of the lavas (initial $\varepsilon Nd = +2.9$) indicate that the Pyke Hill mantle source has experienced previous episodes of melt extraction long before the formation of the komatiite magmas. To assess the impact of the earlier melting events on the source composition in terms of its Re/Os and Pt/Os ratios, the evolution of the Sm–Nd and Re–Os isotope systems in the source were modeled. The abundances of Sm and Nd in the source (Table 5) were calculated from the abundances of these elements in the Pyke Hill lava using the regressions in Fig. A1 as outlined above. Calculations show that in order to increase the $^{147}Sm/^{144}Nd$ ratio in the source of Pyke Hill komatiites by ~30% from the PM value of 0.1967 to its calculated value of 0.2670, the early extracted melt(s) should have formed by ~3% partial melting; that is, it should have been basaltic in composition. For these calculations, a batch melting equation was used; it was assumed that the residue had a composition of garnet lherzolite (65% Ol, 20% Opx, 10% Cpx, 5% Gar), and the bulk partition coefficients for Nd (0.025) and Sm (0.047) were calculated using the compilation of Green [60]. Furthermore, this melting event is calculated to have taken place ~300 Ma before the formation of the Pyke Hill komatiites (i.e., at ~3025 Ma) to allow the source to evolve to the radiogenic Nd isotopic composition with $\varepsilon Nd = +2.9$ by 2725 Ma. At the same time, this melting event is calculated to have decreased the $^{187}Re/^{188}Os$ ratio in the source by <10%. The bulk Re partition coefficient was assumed to be similar to that of Yb, as inferred by Hauri and Hart [61] (0.29; calculated in the same manner as those for Nd and Sm), and the bulk Os partition coefficient was assumed to be >50. Such a decrease in the Re/Os ratio of the source over the time span of 300 Ma will lower its $^{187}Os/^{188}Os$ isotopic composition by ~0.3 gamma

units. This < 10% difference in the Re/Os ratio is about equivalent to the difference in the Re/Os ratio of PUM (0.4346) and that obtained in the previous section for the mantle averaged over the ~ 3.8 Ga Earth history (0.4020). The results of modeling thus indicate that the mantle Re–Os systematics are much less sensitive to the extraction of low-degree partial melts than the Sm–Nd systematics due to a less incompatible behavior of Re compared to Nd. They also indicate that extraction of high-degree partial melts (komatiites) from the mantle will lead to a substantial depletion of the sources in Re (Fig. 6). These sources with time will tend to develop highly unradiogenic $^{187}Os/^{188}Os$ isotopic compositions, which are subsequently observed in samples of subcontinental lithospheric mantle (e.g., [10]). This argument can be also applied to the Pt–Os systematics, keeping in mind that this system has two distinct features. First, Pt is only incompatible during high-degree melting, and therefore the Pt/Os ratio in the source is even less affected by extraction of low-degree melts than the Re/Os ratio. Second, due to the very slow rate at which the Pt–Os isotopic system evolves, very large changes in the Pt/Os ratio (two orders of magnitude larger compared to the Re/Os ratio) in the source are required to develop detectable differences in the $^{186}Os/^{188}Os$ isotopic composition over the same time interval. Thus, it is concluded here that prior melting events have had no effect on the Pt/Os ratios in the Pyke Hill source.

Table 5
PGE, Sm–Nd isotope, and trace element data for Pyke Hill komatiites and their inferred mantle source as compared to PUM

Parameters	Pyke Hill komatiite	Pyke Hill source	PUM
MgO (wt.%)	27.4	38.3	37.8
Re (ppb)	0.47	0.30	0.25
Os	2.38	3.9	3.33
Ir	2.13	3.6	3.30
Ru	5.31	5.4	4.89
Pt	11.1	6.4	6.79
Pd	10.6	6.3	3.84
Nd (ppm)	1.54	0.812	1.19
Sm	0.658	0.385	0.387
Yb	0.868	0.521	0.414
$(La/Sm)_N$	0.42	0.41	= 1
$(Gd/Yb)_N$	0.98	0.93	= 1
Nb/Nb*	1.1	1.1	= 1
$^{147}Sm/^{144}Nd$	0.259	0.267	0.197
$^{190}Pt/^{188}Os$	0.00447	0.00157	0.00157
$^{187}Re/^{188}Os$	0.9510	0.4308	0.4396

Major and trace element data for PUM from [67]. The PGE abundances and the Pt/Os ratio in the Pyke Hill source were calculated from those in the lavas; the Re/Os ratio in the source was obtained from the Re–Os systematics.

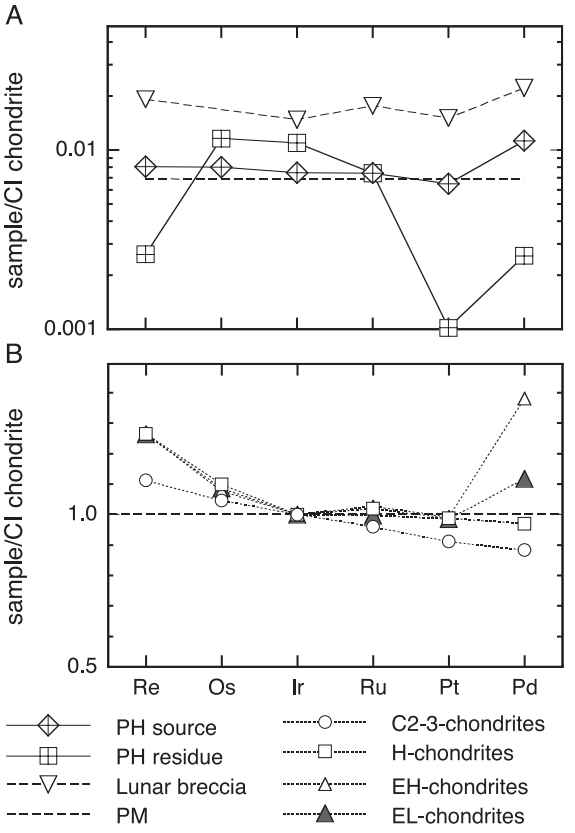

Fig. 6A. CI chondrite-normalized HSE abundances in the calculated mantle source of the Pyke Hill komatiite and in the mantle residue left after the melt extraction. The composition of lunar melt breccias from [62] are shown for comparison. (B) CI chondrite- and Ir-normalized HSE abundances in carbonaceous (C2-3), ordinary (H), and enstatite (EH, EL) chondrites from [63]. Composition of the primitive mantle (broken line) is calculated assuming an Ir content of 3.3 ppb [65] and CI chondrite relative abundances of Anders and Grevesse [66], which were also used as normalizing values.

5.4. Implications for the models of earth accretion and differentiation

The HSE and Pt–Re–Os isotopic data for the Pyke Hill komatiites, and compilation and modeling

presented in the previous sections indicate that since the Archean, the mantle, on average, evolved with near-chondritic Re/Os and Pt/Os ratios and has had HSE abundances similar to those found in the modern mantle. These data can be reconciled with two hypotheses. The HSE pattern in the Pyke Hill source is similar to that in enstatite chondrites (Fig. 6), including the CI-suprachondritic Os/Ir and Pd/Ir ratios. Furthermore, the Re–Os isotope systematics of the Pyke Hill source, too, are similar to those in enstatite and ordinary chondrites. An ordinary or enstatite chondrite veneer as a source of the HSE in the Earth's mantle has been recently proposed by Brandon et al. [6] in their study of abyssal peridotites, by Meisel et al. [47] in their study on mantle xenoliths, and by Norman et al. [62] in their study of lunar impact melts. The latter also have HSE patterns similar to that calculated for the Pyke Hill source (Fig. 6). It should be noted however that although the Pd/Pt ratio in average enstatite chondrites (0.71; [63]) is similar to that in ADSL (0.65), it is ~30% lower than that in the Pyke Hill source (0.99), and average ordinary chondrites have a Pd/Pt ratio (0.56; [63]) that is actually similar to that in CI-chondrites.

Alternatively, the reenrichment of the mantle with HSEs after core separation, observed in the source of the Pyke Hill lavas, could be the result of an open-system transport of material across the core–mantle boundary. To account for the generally chondritic Os isotopic composition of the mantle, it must be assumed that such transport was a global event that occurred before any substantial inner core crystallization had taken place. Current models for the Earth's thermal history place the onset of inner core crystallization between 3.8 and 1.0 Ga depending on the presence of radioactive elements in the core [28,64]. The relatively early (≥3.5 Ga) onset of inner core crystallization is required to explain the radiogenic $^{187}Os/^{188}Os$ isotopic compositions of the Archean Kostomuksha and Belingwe komatiites [50,55], provided that these radiogenic signatures were derived from the outer core, after inner core segregation and subsequent ingrowth of radiogenic Os, as proposed by these authors. As such, the chondritic HSE pattern must have been imprinted very early in Earth history, perhaps at about the time of core formation.

6. Conclusions

1. For the purposes of the HSE abundance and Os isotopic study, the emplaced Pyke Hill komatiite lava represents a pristine mantle melt that was not affected by secondary alteration or crustal contamination.
2. The mantle source of Pyke Hill komatiites was characterized by initial $\gamma^{187}Os = +0.62 \pm 0.15$ and $^{186}Os/^{188}Os = 0.1198318 \pm 18$. The Re–Os isotopic composition is similar to those of enstatite and ordinary chondrites [46].
3. The present-day Re–Os isotopic composition of the Pyke Hill source ($^{187}Os/^{188}Os = 0.1293$, $^{187}Re/^{188}Os = 0.4308$) is identical to that estimated for PUM (0.1296 ± 0.0008, 0.4346). Using the Pt–Os isotopic data for the Pyke Hill komatiite source, the present-day $^{186}Os/^{188}Os$ isotopic composition of PUM was estimated to be 0.1198387.
4. The regression of global $^{187}Os/^{188}Os$ isotopic data for terrestrial materials, unambiguously shown to represent Os isotopic composition of contemporary mantle, indicates that the LILE-depleted mantle averaged over Earth's history evolved from the solar system starting composition and was on average ~8% depleted in Re vs. Os relative to PUM.
5. The much smaller depletions in Re/Os and Pt/Os compared to Nd/Sm in terrestrial mantle sources are attributed to a more compatible behavior of Re and Pt vs. LREE during low degrees of partial melting.
6. The Pyke Hill komatiite source was calculated to contain, in ppb: Re = 0.30, Os = 3.9, Ir = 3.6, Ru = 5.4, Pt = 6.4, and Pd = 6.3. All HSE occur in relative proportions similar to those found in average enstatite chondrites [63] except for Pd, which is enriched over Pt by ~30%. From these abundances, the $^{190}Pt/^{188}Os$ of PUM was inferred to be 0.00157.
7. The HSE abundance and Os isotope data for the Pyke Hill komatiites imply a mantle HSE composition that is consistent with both the models of the accretion of a late veneer and interaction of the mantle with the core after the initial core separation. If the reenrichment of the mantle with HSE was the result of an open-system transport of material across the core–mantle boundary, it was likely to be a global event that should have occurred at about the time of core formation.

Acknowledgements

We thank Mike Lesher and Rebecca Sproule for their guidance in the field and many discussions of the geology of Pyke Hill komatiites. Assistance of Andy Campbell in keeping the element up and running is greatly appreciated. We are indebted to Dmitry Zhuravlev, who provided state-of-the-art analyses of lithophile trace elements, and to Elvira Macsenaere-Riester for major and minor element analyses. We would like to thank Graham Pearson for a thoughtful review and Ken Farley for editorial handling. This study was supported by NSF EAR-0106974 and EAR-0309786 to MH and ISP, and by NSF EAR 0000908 to ADB. These sources of support are gratefully acknowledged. ***[KF]***

Appendix A. Major, minor, and lithophile trace elements

Major, minor, and lithophile trace element data for the studied samples are listed in Table A1 and plotted on MgO variation diagrams in Fig. A1 and as primitive mantle-normalized abundances in Fig. A2. The average MgO content of the upper and lower chilled margins (PH25 and PH34) that represent the composition of the emplaced komatiite lava is 27.4%. The MgO abundances range between 27.4% and 26.8% in the olivine spinifex-textured samples and between 30.6% and 34.7% in the olivine cumulates. Most major, minor, and lithophile trace elements reported in Table A1 show strong correlations with MgO and vary in a manner entirely consistent with fraction-

Table A1
Major (wt.%), minor, and trace element (ppm) data

Sample	PH25	PH26	PH27	PH28	PH29	PH30	PH31	PH32	PH33	PH34
SiO_2	44.8	45.2	44.4	45.4	45.2	44.6	44.9	45.2	45.3	45.8
TiO_2	0.330	0.331	0.352	0.350	0.310	0.261	0.250	0.270	0.279	0.351
Al_2O_3	6.93	6.82	7.06	7.25	6.35	5.27	5.15	5.57	5.87	7.22
Fe_2O_3	12.3	11.8	13.0	11.9	11.3	10.6	10.1	10.4	10.8	11.7
MnO	0.17	0.19	0.19	0.18	0.15	0.11	0.11	0.12	0.12	0.17
MgO	27.8	27.4	26.8	26.8	30.6	34.4	34.7	33.1	31.8	26.9
CaO	6.58	7.49	7.18	6.96	5.09	3.75	3.74	4.40	5.07	6.99
Na_2O	0.43	0.27	0.38	0.50	0.33	0.30	0.29	0.28	0.24	0.40
K_2O	0.05	0.02	0.03	0.06	0.03	0.03	0.09	0.05	0.04	0.03
P_2O_5	0.02	0.01	0.02	0.02	0.01	0.01	0.01	0.01	0.01	0.01
LOI	6.88	6.98	6.72	6.11	7.52	9.04	9.11	8.50	7.64	6.19
Total	100.8	100.8	100.6	100.4	101.0	101.0	101.1	101.0	100.8	100.8
Cr	2759	2670	2812	2782	2494	2390	2349	2409	2450	2887
Ni	1489	1332	1400	1310	1738	2006	1996	1926	1799	1330
Zr	16.2	16.1	17.4	17.6	14.6	12.3	11.9	12.8	14.0	17.2
Nb	0.413	0.421	0.438	0.439	0.360	0.304	0.310	0.322	0.348	0.444
Y	8.18	8.35	8.76	8.72	7.43	6.14	6.08	6.44	7.03	8.56
Ga	6.80	6.95	7.07	7.45	6.20	5.22	4.80	5.30	5.81	7.36
Th	0.042	0.043	0.044	0.043	0.035	0.029	0.028	0.031	0.034	0.042
La	0.434	0.439	0.464	0.458	0.383	0.321	0.327	0.344	0.369	0.443
Ce	1.39	1.44	1.51	1.44	1.23	1.06	1.04	1.08	1.19	1.43
Nd	1.49	1.57	1.64	1.63	1.36	1.11	1.12	1.18	1.29	1.58
Sm	0.639	0.653	0.682	0.666	0.590	0.491	0.464	0.519	0.544	0.678
Eu	0.268	0.269	0.282	0.297	0.227	0.216	0.195	0.212	0.217	0.265
Gd	1.01	1.03	1.08	1.09	0.938	0.753	0.734	0.796	0.875	1.08
Dy	1.30	1.32	1.38	1.38	1.16	0.968	0.936	1.03	1.13	1.41
Er	0.857	0.879	0.929	0.911	0.801	0.654	0.629	0.673	0.749	0.911
Yb	0.847	0.873	0.892	0.904	0.791	0.646	0.635	0.665	0.715	0.888
$(La/Sm)_n$	0.43	0.42	0.43	0.43	0.41	0.41	0.44	0.42	0.43	0.41
$(Gd/Yb)_n$	0.97	0.95	0.98	0.97	0.96	0.94	0.93	0.97	0.99	0.99
Nb/Nb*	1.11	1.12	1.11	1.13	1.12	1.14	1.18	1.12	1.13	1.19

Abundances are recalculated on an anhydrous basis. Major and minor (Cr, Ni) element data for all samples, except PH34, from [29].

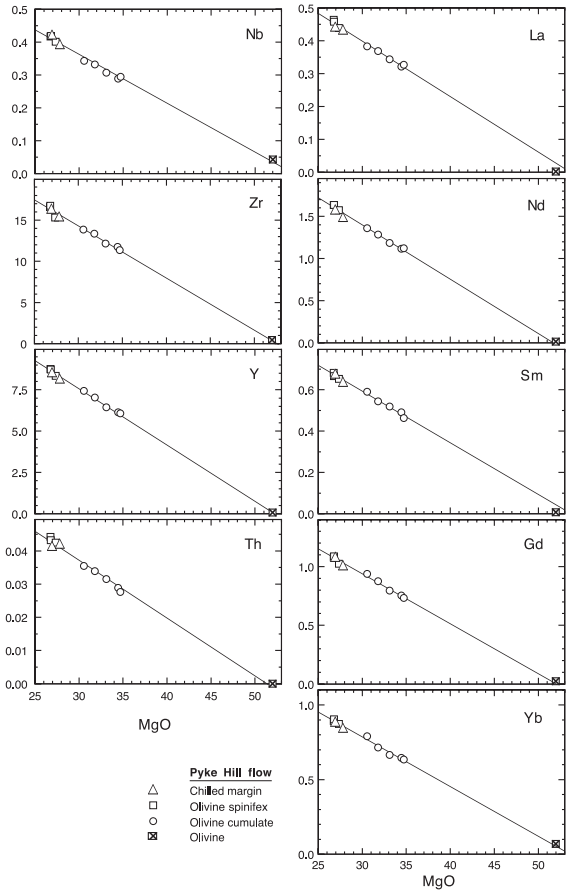

Fig. A1. Variation diagrams of MgO (wt.%) vs. selected lithophile trace elements for the PH-II komatiite flow. The linear trends are best fit lines through the data points. The trace element composition of the olivine was calculated using the composition of the emplaced komatiite lava from which this olivine crystallized and $D^{Ol\text{-}Liq}$ from [60].

ation/accumulation of olivine, the only major liquidus phase. When plotted against MgO, the data fall on the olivine control lines that intersect the MgO axes at ~ 52% MgO and pass through the calculated liquidus olivine compositions, indicating that these elements were immobile during alteration on the scale of the drill core samples. The rocks are strongly depleted in highly incompatible LILE, including LREE and Th [$(La/Sm)_n = 0.42$, $(Th/La)_n = 0.70$], exhibit positive Nb anomalies ($Nb/Nb^* = 1.1$), and have near-chondritic ratios of moderately incompatible elements [$(Al/Ti)n = 0.92$, $(Gd/Yb)_n = 0.98$].

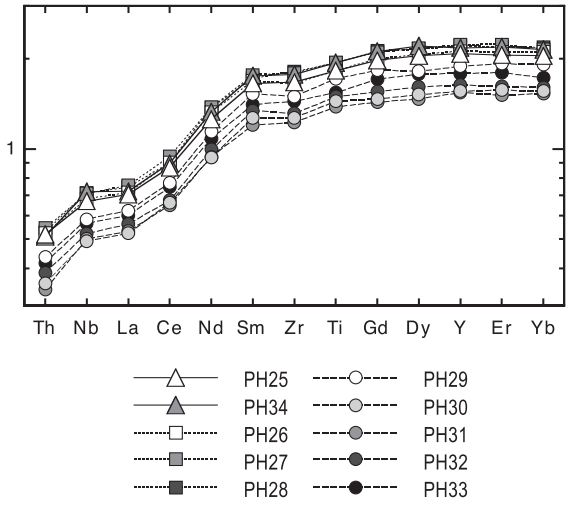

Fig. A2. Abundances of selected major and trace elements in the Pyke Hill komatiite flow normalized to primitive mantle values of Hofmann [67].

References

[1] R.J. Walker, J.W. Morgan, E.S. Beary, M.I. Smoliar, G.K. Czamanske, M.F. Horan, Applications of the $^{190}Pt-^{186}Os$ isotope system to geochemistry and cosmochemistry, Geochim. Cosmochim. Acta 61 (1997) 4799–4807.

[2] S.B. Shirey, R.J. Walker, The Re–Os isotope system in cosmochemistry and high-temperature geochemistry, Annu. Rev. Earth Planet. Sci. 26 (1998) 423–500.

[3] T. Meisel, J. Moser, W. Wegscheider, Recognizing heterogenous distribution of platinum group elements (PGE) in geological materials by means of the Re–Os isotope system, Fresenius' J. Anal. Chem. 370 (2001) 566–572.

[4] R.J. Walker, H.M. Prichard, A. Ishivatari, M. Pimentel, The osmium isotopic composition of the convecting upper mantle deduced from ophiolite chromites, Geochim. Cosmochim. Acta 66 (2002) 329–345.

[5] J.E. Snow, L. Reisberg, Os isotopic systematics of the MORB mantle: results from altered abyssal peridotites, Earth Planet. Sci. Lett. 136 (1995) 723–733.

[6] A.D. Brandon, J.E. Snow, R.J. Walker, J.W. Morgan, T.D. Mock, $^{190}Pt-^{186}Os$ and $^{187}Re-^{187}Os$ systematics of abyssal peridotites, Earth Planet. Sci. Lett. 177 (2000) 319–335.

[7] P. Schiano, J.-L. Birck, C.J. Allégre, Osmium–strontium–neodymium–lead isotopic covariations in mid-ocean ridge basalt glasses and the heterogeneity of the upper mantle, Earth Planet. Sci. Lett. 150 (1997) 363–379.

[8] M. Roy-Barman, G.J. Wasserburg, D.A. Papanastassiou, M. Chaussidon, Osmium isotopic compositions and Re–Os concentrations in sulfide globules from basaltic glasses, Earth Planet. Sci. Lett. 154 (1998) 331–347.

[9] L. Reisberg, J.-P. Lorand, Longevity of subcontinental mantle

lithosphere from osmium isotope systematics in orogenic peridotite massifs, Nature 376 (1995) 159–162.
[10] D.G. Pearson, G.J. Irvine, D.A. Ionov, F.R. Boyd, G.E. Dreibus, Re–Os isotope systematics and platinum-group-element fractionation during mantle melt extraction: a study of peridotite xenoliths from N. Lesotho and S. Namibian kimberlites, the Vitim volcanic field and massif peridotites from Beni Bousera, Chem. Geol. (2004) (in press).
[11] A.E. Saal, R.L. Rudnick, G.E. Ravizza, S.R. Hart, Re–Os isotope evidence for the composition, formation and age of the lower continental crust, Nature 393 (1998) 58–61.
[12] R.J. Walker, E. Hanski, J. Vuollo, J. Liipo, The Os isotopic composition of Proterozoic upper mantle: evidence for chondritic upper mantle from the Outokumpu ophiolite, Finland, Earth Planet. Sci. Lett. 141 (1996) 161–173.
[13] J.G. Foster, D.D. Lambert, L.R. Frick, R. Maas, Re–Os isotopic evidence for genesis of Archaean nickel ores from uncontaminated komatiites, Nature 382 (1996) 703–706.
[14] S.B. Shirey, Initial Os isotopic composition of Munro Township, Ontario komatiites revisited: additional evidence for near-chondritic, late-Archaean convecting mantle beneath the Superior Province, 7th V.M. Goldschmidt Conference Abstr., 1997, p. 193.
[15] I.S. Puchtel, G.E. Brügmann, A.W. Hofmann, Precise Re–Os mineral isochron and Pb–Nd–Os isotope systematics of a mafic–ultramafic sill in the 2.0 Ga Onega plateau (Baltic Shield), Earth Planet. Sci. Lett. 170 (1999) 447–461.
[16] A. Tsuru, R.J. Walker, A. Kontinen, P. Peltonen, E. Hanski, Re–Os isotopic systematics of the 1.95 Ga Jormua Ophiolite Complex, northeastern Finland, Chem. Geol. 164 (2000) 123–141.
[17] I.S. Puchtel, G.E. Brügmann, A.W. Hofmann, V.S. Kulikov, V.V. Kulikova, Os isotope systematics of komatiitic basalts from the Vetreny belt, Baltic Shield: evidence for a chondritic source of the 2.45 Ga plume, Contrib. Mineral. Petrol. 140 (2001) 588–599.
[18] V.C. Bennett, A.P. Nutman, T.M. Esat, Constraints on mantle evolution from $^{187}Os/^{188}Os$ isotopic compositions of Archean ultramafic rocks from southern West Greenland (3.8 Ga) and Western Australia (3.46 Ga), Geochim. Cosmochim. Acta 66 (2002) 2615–2630.
[19] A. Gangopadhyay, R.J. Walker, Re–Os systematics of the ca. 2.7 Ga komatiites from Alexo, Ontario, Canada, Chem. Geol. 196 (2003) 147–162.
[20] E. Hanski, R.J. Walker, G.V. Polyakov, A.I. Glotov, P.A. Balykin, T.T. Hoa, N.T. Phuong, Permian–Triassic komatiites and their Os isotopic characteristics in northwestern Vietnam, 12th V.M. Goldschmidt Conference Abstr., 2002, p. A309.
[21] A.H. Wilson, S.B. Shirey, R.W. Carlson, Archaean ultra-depleted komatiites formed by hydrous melting of cratonic mantle, Nature 423 (2003) 858–860.
[22] A. Gangopadhyay, R.J. Walker, E. Hanski, P. Solheid, Origin of Paleoproterozoic Tienriched komatiitic rocks from Jeesiörova, Kittilä greenstone complex, Finnish Lapland, J. Petrol. (2004) (in press).
[23] A.D. Brandon, R.J. Walker, J.W. Morgan, M.D. Norman, H.M. Prichard, Coupled ^{186}Os and ^{187}Os evidence for core–mantle interaction, Science 280 (1998) 1570–1573.
[24] A.D. Brandon, The osmium isotopic composition of Tagish Lake and other chondrites, implications for late terrestrial planetary accretion, Lunar Planet. Sci. XXXIV (2003) 1776.
[25] A.D. Brandon, M.D. Norman, R.J. Walker, J.W. Morgan, $^{186}Os–^{187}Os$ systematics of Hawaiian picrites, Earth Planet. Sci. Lett. 174 (1999) 25–42.
[26] A.D. Brandon, R.J. Walker, I.S. Puchtel, H. Becker, M. Humayun, S. Revillon, $^{186}Os–^{187}Os$ systematics of Gorgona Island komatiites: implications for early growth of the inner core, Earth Planet. Sci. Lett. 206 (2003) 411–426.
[27] B.A. Buffett, H.E. Huppert, J.R. Lister, A.W. Woods, On the thermal evolution of the Earth's core, J. Geophys. Res. 101 (1996) 7989–8006.
[28] S. Labrosse, J.-P. Poirier, J.-L. Le Mouël, The age of the inner core, Earth Planet. Sci. Lett. 190 (2001) 111–123.
[29] I.S. Puchtel, M. Humayun, A. Campbell, R. Sproule, C.M. Lesher, Platinum group element geochemistry of komatiites from the Alexo and Pyke Hill areas, Ontario, Canada, Geochim. Cosmochim. Acta 68 (2004) 1361–1383.
[30] R.A. Sproule, C.M. Lesher, J.A. Ayer, P.C. Thurston, C.T. Herzberg, Spatial and temporal variations in the geochemistry of komatiites and komatiitic basalts in the Abitibi greenstone belt, Precambrian Res. 115 (2002) 153–186.
[31] D.R. Pyke, A.J. Naldrett, O.R. Eckstrand, Archean ultramafic flows in Munro Township, Ontario, Geol. Soc. Amer. Bull. 84 (1973) 955–978.
[32] I.S. Puchtel, M. Humayun, PGE fractionation in a komatiitic basalt lava lake, Geochim. Cosmochim. Acta 17 (2001) 2979–2993.
[33] K.R. Ludwig, ISOPLOT—a plotting and regression program for radiogenic isotope data, version 2.95, Open File Rep. – U.S. Geol. Surv. 91–445 (1997) 47 pp.
[34] F. Begemann, K.R. Ludwig, G.W. Lugmair, K. Min, L.E. Nyquist, P.J. Patchett, P.R. Renne, C.-Y. Shih, I.M. Villa, R.J. Walker, Call for an improved set of decay constants for geochronological use, Geochim. Cosmochim. Acta 65 (2001) 111–121.
[35] M.I. Smoliar, R.J. Walker, J.W. Morgan, Re–Os ages of Group IIA, IIIA, IVA, and IVB iron meteorites, Science 271 (1996) 1099–1102.
[36] J.A. Ayer, Y. Amelin, F. Corfu, S. Kamo, J. Ketchum, K. Kwok, N. Trowell, Evolution of the southern Abitibi greenstone belt based on U–Pb geochronology: autochthonous volcanic construction followed by plutonism, regional deformation and sedimentation, Precambrian Res. 115 (2002) 63–95.
[37] B. Dupré, C. Chauvel, N.T. Arndt, Pb and Nd isotopic study of two Archean komatiitic flows from Alexo, Ontario, Geochim. Cosmochim. Acta 48 (1984) 1965–1972.
[38] R.J. Walker, S.B. Shirey, O. Stecher, Comparative Re–Os, Sm–Nd and Rb–Sr isotope and trace element systematics for Archean komatiite flows from Munro Township, Abitibi belt, Ontario, Earth Planet. Sci. Lett. 87 (1988) 1–12.
[39] Y. Lahaye, N.T. Arndt, Alteration of a komatiite flow from Alexo, Ontario, J. Petrol. 37 (1996) 1261–1284.
[40] J. Carignan, N. Machado, C. Gariépy, U–Pb isotopic geochemistry of komatiites and pyroxenes from the southern Abitibi greenstone belt, Canada, Chem. Geol. 126 (1995) 17–27.

[41] K. Righter, A.J. Campbell, M. Humayun, R.L. Hervig, Partitioning of Re, Ir, Rh, and Ru between Cr-bearing spinels, olivine, pyroxene and silicate melts, Geochim. Cosmochim. Acta 68 (2004) 867–880.
[42] J.M. Brenan, W.F. McDonough, C. Dalpé, Experimental constraints on the partitioning of rhenium and some platinum-group elements between olivine and silicate melt, Earth Planet. Sci. Lett. 212 (2003) 135–150.
[43] N.T. Arndt, Komatiites: a dirty window to the Archean mantle, Terra Cogn. 6 (1986) 59–66.
[44] I.S. Puchtel, K.M. Haase, A.W. Hofmann, C. Chauvel, V.S. Kulikov, C.-D. Garbe- Schönberg, A.A. Nemchin, Petrology and geochemistry of crustally contaminated komatiitic basalts from the Vetreny Belt, southeastern Baltic Shield: evidence for an Early Proterozoic mantle plume beneath rifted Archean continental lithosphere, Geochim. Cosmochim. Acta 61 (1997) 1205–1222.
[45] E.G. Nisbet, M.J. Cheadle, N.T. Arndt, M.J. Bickle, Constraining the potential temperature of the Archaean mantle: a review of the evidence from komatiites, Lithos 30 (1993) 291–307.
[46] R.J. Walker, M.F. Horan, J.W. Morgan, H. Becker, J.N. Grossman, A.E. Rubin, Comparative ^{187}Re–^{187}Os systematics of chondrites: implications regarding early solar system processes, Geochim. Cosmochim. Acta 66 2002, pp. 4187–4201.
[47] T. Meisel, R.J. Walker, A.J. Irving, J.-P. Lorand, Osmium isotopic compositions of mantle xenoliths: a global perspective, Geochim. Cosmochim. Acta 65 (2001) 1311–1323.
[48] J.W. Morgan, R.J. Walker, M.F. Horan, E.S. Beary, A.J. Naldrett, ^{190}Pt–^{186}Os and ^{187}Re–^{187}Os systematics of the Sudbury Igneous Complex, Ontario, Geochim. Cosmochim. Acta 66 (2002) 273–290.
[49] D.L. Cook, R.J. Walker, M.F. Horan, J.T. Wasson, J.W. Morgan, Pt–Re–Os systematics of Group IIAB and IIIAB iron meteorites, Geochim. Cosmochim. Acta 68 (2004) 1413–1431.
[50] R.J. Walker, E. Nisbet, ^{187}Os isotopic constraints on Archean mantle dynamics, Geochim. Cosmochim. Acta 66 (2002) 3317–3325.
[51] R.J. Walker, L.M. Echeverria, S.B. Shirey, M.F. Horan, Re–Os isotopic constraints on the origin of volcanic rocks, Gorgona Island, Colombia: Os-isotopic evidence for ancient heterogeneities in the mantle, Contrib. Mineral. Petrol. 107 (1991) 150–162.
[52] R.J. Walker, J.W. Morgan, E. Hanski, V.F. Smolkin, Re–Os systematics of Early Proterozoic picrites, Pechenga complex, NW Russia: evidence for ancient ^{187}Os-enriched plumes, Geochim. Cosmochim. Acta 61 (1997) 3145–3160.
[53] S.B. Shirey, K.W. Lewin, J.H. Berg, R.W. Carlson, Temporal changes in the sources of flood basalts: isotopic and trace element evidence from the 1100 Ma old Keweenawan Mamainse Point Formation, Ontario, Canada, Geochim. Cosmochim. Acta 58 (1994) 4475–4490.
[54] M.F. Horan, R.J. Walker, V.A. Fedorenko, G.K. Czamanske, Osmium and neodymium isotopic constraints on the temporal and spatial evolution of Siberian flood basalt sources, Geochim. Cosmochim. Acta 59 (1995) 5159–5168.
[55] I.S. Puchtel, G.E. Brügmann, A.W. Hofmann, ^{187}Os-enriched domain in an Archaean mantle plume: evidence from 2.8 Ga komatiites of the Kostomuksha greenstone belt, NW Baltic Shield, Earth Planet. Sci. Lett. 186 (2001) 513–526.
[56] R.J. Walker, J.W. Morgan, M.F. Horan, ^{187}Os enrichment in some plumes: evidence for core–mantle interaction, Science 269 (1995) 819–822.
[57] J.C. Lassiter, E.H. Hauri, Osmium–isotope variations in Hawaiian lavas: evidence for recycled oceanic lithosphere in the Hawaiian plume, Earth Planet. Sci. Lett. 164 (1998) 483–496.
[58] R.J. Walker, W.E. Stone, Os isotope constraints on the origin of the 2.7 Ga Boston Creek Flow, Ontario, Canada, Chem. Geol. 175 (2001) 567–579.
[59] I.S. Puchtel, 3.0 Ga Olondo greenstone belt in the Aldan Shield, E. Siberia, in: T.M. Kusky, K.C. Condie (Eds.), Precambrian Ophiolites and related rocks, Elsevier, Amsterdam, 2004, in press.
[60] T.H. Green, Experimental studies of trace-element partitioning applicable to igneous petrogenesis—Sedona 16 years later, Chem. Geol. 117 (1994) 1–36.
[61] E.H. Hauri, S.R. Hart, Rhenium abundances and systematics in oceanic basalts, Chem. Geol. 139 (1997) 185–205.
[62] M.D. Norman, V.C. Bennett, G. Ryder, Targeting the impactors: siderophile element signatures of lunar impact melts from Serenitatis, Earth Planet. Sci. Lett. 202 (2002) 217–228.
[63] M.F. Horan, R.J. Walker, J.W. Morgan, J.N. Grossman, A.E. Rubin, Highly siderophile elements in chondrites, Chem. Geol. 196 (2003) 5–20.
[64] B.A. Buffett, The thermal state of Earth's core, Science 299 (2003) 1675–1676.
[65] J.W. Morgan, Ultramafic xenoliths: clues to Earth's late accretionary history, J. Geophys. Res. 91 (1986) 12375–12387.
[66] E. Anders, N. Grevesse, Abundances of the elements: meteoritic and solar, Geochim. Cosmochim. Acta 53 (1989) 197–214.
[67] A.W. Hofmann, Chemical differentiation of the Earth: the relationship between mantle, continental crust and oceanic crust, Earth Planet. Sci. Lett. 90 (1988) 297–314.